Design and Analysis of an Axially Laminated Reluctance Motor for Variable-Speed Applications

Esra Kandemir BESER, Sabri CAMUR, Birol ARIFOGLU, Ersoy BESER
Kocaeli University, Department of Electrical Electircal Engineering, 41380, Turkey
esrakandemir@kocaeli.edu.tr

***Abstract*—In this paper, an axially laminated reluctance motor is presented. First, a set of a finite element analysis (FEA) on three different axially laminated rotor geometries was carried out and torque profiles of the rotors were predicted. The effect of the stator slot skewing on the torque profiles were also examined in the analysis. After deciding the rotor geometry, the mathematical model of the proposed motor was formed in terms of a,b,c variables and simulations were performed. Motor prototype and motor drive were introduced. Torque profiles of the motor were measured for different current values and load test were realized. Experimental results were compared to analysis and simulation results. There is a good accordance between experimental and simulation results. When the proposed motor is operated with electrical 120° mode as a brushless DC motor, the torque versus speed characteristic shows a DC series motor characteristic and speed of the motor can be easily controlled by regulating the bus voltage. These features make the proposed motor convenient for variable-speed applications such as electrical vehicles.**

***Index Terms*—axially laminated rotor, brushless motors, magnetic analysis, reluctance motor, variable speed drives.**

I. INTRODUCTION

Variable-speed applications have been gradually increasing through the existing demand in the industry. Therefore, the studies have been continuing in order to develop new motors and drive systems. Permanent magnet and reluctance motors constitute two popular topics in the literature.

Reluctance motors can be classified as switched reluctance motors (SRMs) and synchronous reluctance motors (SynRMs). These motor types do not include magnets or winding on their rotors. There is no demagnetization risk and it makes them suitable for using at high temperatures [1]. In absence of rotor currents, produced torque is independent from rotor temperature. Saturation at high current values is a drawback of these motors.

Stator and rotor structures are designed providing salient poles in SRM and pole numbers are not equal in stator and rotor. Concentrated winding is used in stator poles. SRMs are generally manufactured with a few numbers of pole pairs. SRM has large torque pulsations resulting in noisy operation. SynRM has a distributed winding, stator and rotor pole numbers are equal. General rotor types designed as salient pole, axially and transversally laminated in SynRM.

SynRMs have been discussed in various studies in the literature. Since the adoption of vector-controlled drives, these machines can represent a viable alternative to other types of ac motors, such as induction or permanent magnet (PM) synchronous ones [2]. SRM has a simple structure when compared with other types of AC machines. The stator of a SRM is similar to that of an induction motor but it has significantly different rotor structures [3].

The performance of synchronous reluctance machines is affected by the values of the inductances of the direct and quadrature axis [4-5]. A very high d-axis inductance (L_d) and a low q-axis inductance (L_q) are required. The ratio of the d and q axis inductances are mentioned as the saliency ratio and this ratio is tried to be possibly high in the synchronous reluctance motors [6-9]. These machine types achieve a wide constant power region and a high power factor, providing a large saliency ratio [10-11].

A large saliency ratio can be constituted by both axially and transversally laminated rotor structures [4], [10-12]. Both lamination types have their advantages and drawbacks [13-14]. The axially laminated rotor possesses better anisotropy than the transversely laminated ones especially for machines with a few number of pole pairs [4].

In recent years, the axially laminated reluctance motor has received growing interest and its usage in servo drive applications has been increased [15]. The rotor of an axially laminated reluctance machine is obtained by stacking steel laminations with nonmagnetic insulation sheets, then assembling them to obtain different reluctances on the q and d-axes [15-17]. An axially laminated rotor offers a very effective approach to flux barrier design, and the attention on the design optimization to achieve a high saliency ratio has increased [18-20].

The main purpose of this paper is to realize analysis and design of an axially laminated reluctance motor. Description of the motor structure is explained in Section 2, in detail. Different rotor types are investigated by FEA in Section 3 and then simulations are performed in Section 4. In Section 5, motor and motor drive are introduced, measurements of the torque profiles are realized and loaded tests are performed on the proposed motor prototype. Considerable results of the simulations and experimental study are presented and discussed in Section 6. Finally, complete paper is evaluated in Section7.

II. DESCRIPTION OF MOTOR STRUCTURE

In this study, axially laminated rotor type is preferred for the rotor of the reluctance machine. In order to produce the reluctance torque, magnetic paths are formed for passing the

Digital Object Identifier 10.4316/AECE.2013.01013

stator magnetic flux through the rotor easily and on the other hand barriers are formed for preventing the flux flow. This process was provided by aligning the magnetic and non-magnetic materials sequentially in the proposed axially laminated rotor type. Thus, minimum inductance value (L_q) is occurred for a rotor position and maximum inductance value (L_d) is obtained by rotation of the rotor by electrically 90°. The ratio between L_d and L_q is significantly affects the reluctance torque. The drawing of an axially laminated rotor type is shown in Fig. 1.

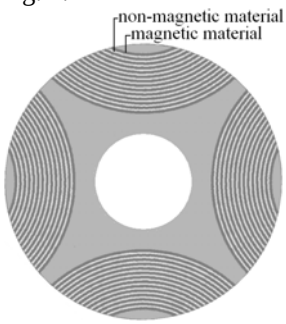

Figure 1. The drawing of an axially laminated rotor type

The insulation ratio (W_{ins}) is mentioned to determine the thickness of both magnetic and non-magnetic materials. W_{ins} is defined as

$$W_{ins} = \frac{W_{non}}{W_{non} + W_{mag}} \quad (1)$$

where W_{non} is the sum of the thickness of the non-magnetic material and W_{mag} is the sum of the thickness of the magnetic material [10-11], [21]. This value affects the saliency ratio and it is recommended as 0.33 in [22], 0.5 in [23-24], 0.4-0.6 in [10-11] and 0.33-0.4 in [25] to obtain the maximum torque value.

Minimum air-gap length is demanded for reluctance machines but providing this procedure is limited by the manufacturing limits. So the feasible air-gap length was preferred as 0.35mm for the analysis and manufacturing process. A conventional stator lamination of an induction motor was used for the considered motor. Some of the considerable dimensions and specifications of the stator and rotor are given in Table I.

TABLE I. DIMENSIONS AND SPECIFICATIONS OF THE STATOR AND ROTOR

Stator	
Outer diameter	200 mm
Number of poles	4
Inner diameter	125 mm
Number of slots	36
Winding	Distributed, 8 turns, star
Stack length	240 mm
Lamination material	M400-50 A
Rotor	
Diameter	124.3 mm
Magnetic material	Grain oriented M6
Non-magnetic material	Aluminum

III. Prediction of Torque Profiles in The Proposed Motor by Finite Element Analysis

The design of the proposed motor is carried out based on the study of torque profiles. Two-dimensional (2D) finite element (FE) software is used to determine the torque waveforms. Various variables of the motor structure affect the produced torque. However, the considered parameters here are the thickness of magnetic and non-magnetic materials and stator slot skewing.

The design is realized according to the dimensions and specifications of the stator and an axially laminated rotor structure in Table I. Dimensions and specifications of the stator design are kept constant in the simulations, only the torque data is modified according to the stator slot skewing.

Three different axially laminated rotor geometries were examined in the FE simulations. Structural specifications of the rotors are given in Table II.

TABLE II. DIMENSIONS AND SPECIFICATIONS OF THE STATOR AND ROTOR

	Rotor A	**Rotor B**	**Rotor C**
Magnetic material thickness	1 mm	1 mm	1 mm
Non-magnetic material thickness	3 mm	1 mm	0.5 mm
Number of magnetic layers	8	14	18
Number of non-magnetic layers	7	13	17
Insulation ratio	0.72	0.48	0.32

After the motors have been modeled, FE analysis is performed by feeding two stator windings with a constant current of 20 A and the torque data is recorded during each rotor movement of 5 mechanical degrees. Views of the investigated motors and flux plots in the simulation program are shown in Fig. 2.

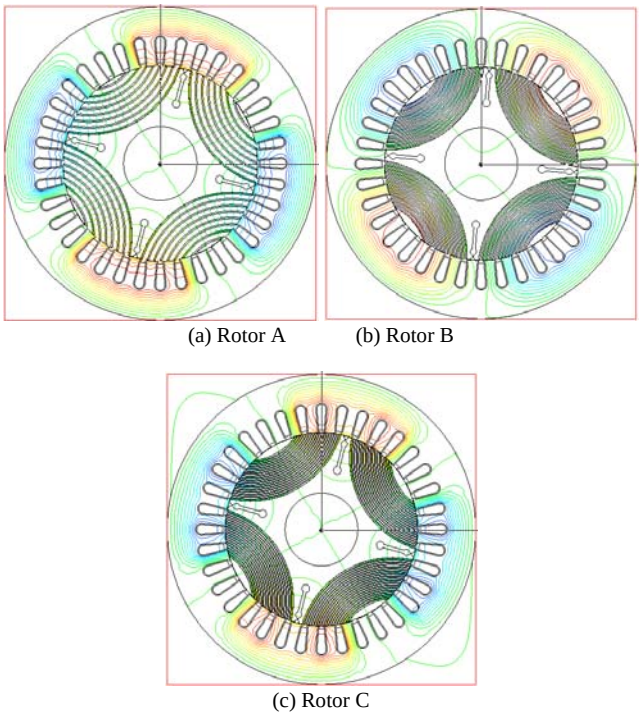

(a) Rotor A (b) Rotor B

(c) Rotor C

Figure 2. View of the investigated motors and flux plot

After obtaining the torque data, the values are arranged providing the different stator slot skewing angles (α_s) for three rotor types. Thus the generated torque versus rotor angle curves are computed and the effect of the thickness of

magnetic and non-magnetic materials and the effect of stator slot skewing on the torque profiles are investigated for the axially laminated reluctance motor. Fig. 3 shows the torque versus rotor angle curves of the Rotor A, B and C at the current value of 20 A, when the stator slots are not skewed and skewed with the angles of 10˚, 15˚ and 40˚ (mechanical).

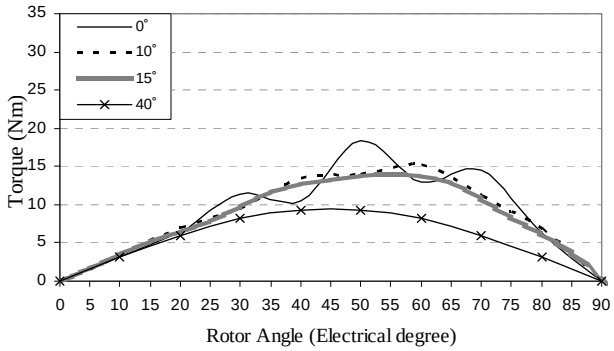

(a)

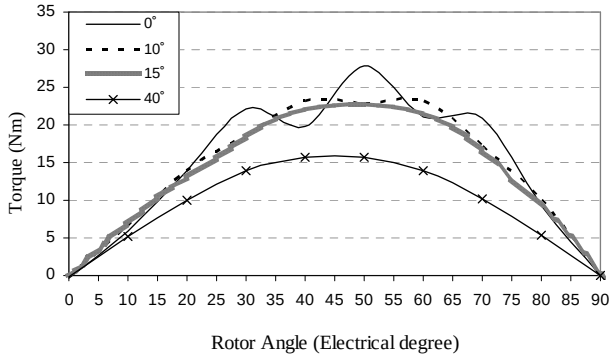

(b)

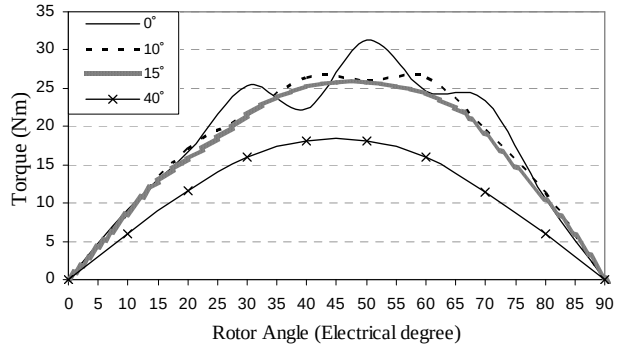

(c)

Figure 3. Calculated torque versus rotor angle curves of the considered rotors for different α_s (I=20 A) (a) Rotor A (b) Rotor B (c) Rotor C

As it can be seen in Fig. 3, stator slot skewing eliminates the torque ripples and smoothes the torque profiles for considered rotor types. However, over skewing of the stator slots affects the torque characteristic negatively and reduces the produced torque. It also causes an unnecessary coil length in the slots. Evaluating the results of FE analysis, α_s of 15˚ seems suitable in point of ripple and maximum value of the torque profile for the three rotor structures. In Fig. 4, torque versus rotor angle characteristics of the rotors are comparatively given for α_s of 15°.

As it can be seen from Fig. 4 that maximum torque value is obtained with the Rotor C. However, some problems can be occurred during the mechanical procedure since the thickness of non-magnetic material is quite thin. In order to prevent the probable problems, the Rotor B is chosen as the prototype machine due to its closest torque profile compared to the Rotor C.

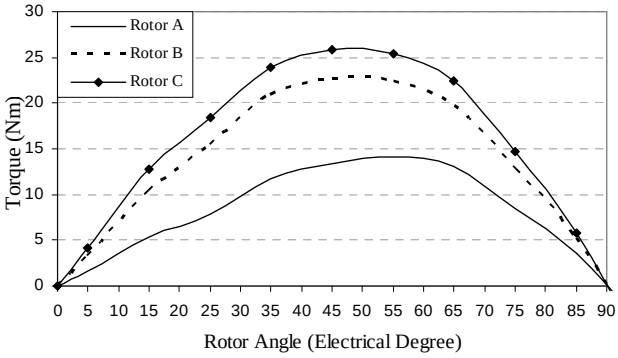

Figure 4. Calculated torque versus rotor angle curves of the considered rotors for α_s of 15°(I=20 A)

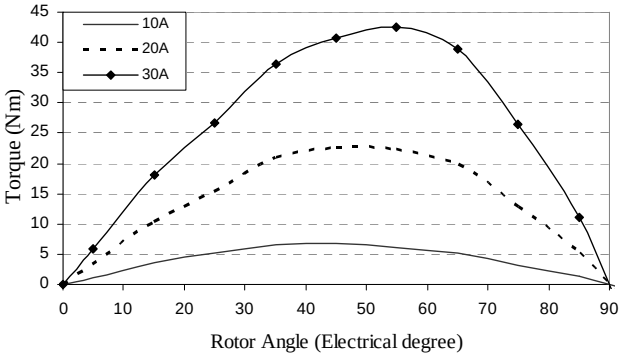

Figure 5. Calculated torque versus rotor angle curves of the Rotor B at different current values for α_s of 15°

After determining α_s and axially laminated rotor type, FE analysis is performed at the current values of 10 A, 20 A and 30 A for the Rotor B. Fig. 5 presents the torques profiles of the Rotor B at different current values.

IV. Mathematical Model and Simulations

Mathematical equations of the reluctance motor can be formed in terms of a,b,c phase variables. The voltage equations of the reluctance machine can be expressed in matrix form as

$$[V]_{a,b,c} = [R]_{a,b,c}[I]_{a,b,c} + [L]_{a,b,c}\frac{d[I]_{a,b,c}}{dt} + \frac{\partial[L]_{a,b,c}}{\partial\theta_r}[I]_{a,b,c}\,\omega_r \quad (2)$$

The electromagnetic torque can also be given as

$$T_e = p\left\{\frac{1}{2}[I]^T{}_{a,b,c}\frac{\partial[L]_{a,b,c}}{\partial\theta_r}[I]_{a,b,c}\right\} \quad (3)$$

where

[V] phase-neutral voltages;
[I] phase currents;
[R] resistance matrix;
[L] inductance matrix;
θ_r rotor position;
ω_r angular velocity;
T_e electromagnetic torque;
p the number of pole pairs.

Mathematical equations were configured and machine parameters were included into the machine model in the simulation program. Stator winding resistance (R_s) was defined as 0.24 Ω for each winding. Self inductance (L_{aa}) and mutual inductance (L_{ab}) were identified from FE simulations as a function of the rotor position as

$$L_{aa}(\theta_r) = 12.7 + 9.8\cos(2\theta_r) - 0.8\sin(2\theta_r)mH \quad (4)$$

$$L_{bc}(\theta_r) = -4.3 + 9.6\cos(2\theta_r) - 0.3\sin(2\theta_r)mH \quad (5)$$

In order to complete the motor system, motor drive and switching algorithm should be added to the simulation program. Phase voltages are produced by using the inverter model having six semiconductor switching elements and the switching algorithm. In the simulation study, Matlab/Simulink environment has been used in order to configure machine and inverter models.

Switching algorithm is based on the operation method of a brushless DC motor. Six switching states are constituted in one electrical period. Two stator windings are activated in each state. Therefore the motor is fed by an inverter synchronized with the rotor position. Switching sequence of the semiconductor elements are modified in each step according to the rotor position data. Reluctance rotor tends to minimum reluctance position and moves to this point by switching process depending on the rotor position. Reluctance torque reaches the maximum value in the middle of the maximum and minimum reluctance points. Due to this periodical operation, the motor realizes the torque production. Reluctance motor resembles a DC series motor by this operation mode since the magnetic flux which is a parameter for the torque production is generated by the stator current and motor torque is proportional to the square of the stator current.

After configuring the mathematical model of the motor and drive system, simulations are realized at different load torques. Simulated phase voltage and current waveforms are given in Fig. 6 for the load torque of 9 Nm.

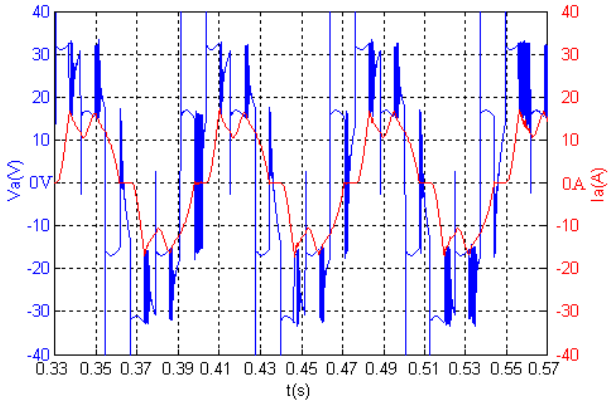

Figure 6. Simulation results of phase voltage and current waveforms at 9 Nm for the proposed motor

Speed versus torque curve is also obtained by increasing the load torque up to 15 Nm. Simulated speed versus torque characteristic is presented together with the experimental curve in Fig. 12. The efficiency is also calculated as 84.4% at the load torque of 9 Nm.

V. Experimental Study

A. Motor Prototype and Motor Drive

After determining the rotor geometry (Rotor B) through the FE analysis, the motor prototype was manufactured considering the design information in Table I. The photograph of the motor body and axially laminated rotor structure is shown in Fig. 7.

The axially laminated reluctance motor was operated by a motor drive synchronized with the rotor position. Motor drive consists of power and control parts. Six N-channel MOSFETs (IXTQ50N20P-200V, 50A) have been used in the power part. Control part includes a microcontroller (18F452), an EPROM (27C256) and MOSFET drivers (IR2118).

Figure 7. The prototype of the motor body and axially laminated rotor structure

Rotor position was sensed by three Hall effect sensors and the data is transferred to the control system of the motor drive to energize the stator windings in proper duration. Switching sequence of the semiconductor elements are modified in each step according to the rotor position. Six different switching states are occurred in one electrical rotation of the rotor.

As it was mentioned in Section 4, when the rotor rotates by 60° electrical, stator current distribution is modified in each state. Motor drive and rotor position sensing system perform the same function with the commutator and brushes in direct current motors. Thus, mechanically commutation in DC machines turns into electronically commutation by this control strategy.

B. Measurement of Torque Profiles

In order to obtain torque versus rotor angle profiles, the proposed motor was tested on a machine test bench. The test equipment has a disc brake to prevent the rotor movement and a torque sensor to measure the generated static torque value. The photograph of the test bench is shown in Fig. 8.

Figure 8. Machine test bench together with the proposed motor

Two stator windings were fed by fixed currents of 10 A, 20 A and 30 A with the aid of a regulated DC source. The rotor was locked by the disc brake and the produced torque

was measured. This process was repeated during the steps of 5 mechanical degrees and torque versus rotor angle curves were obtained for different current values.

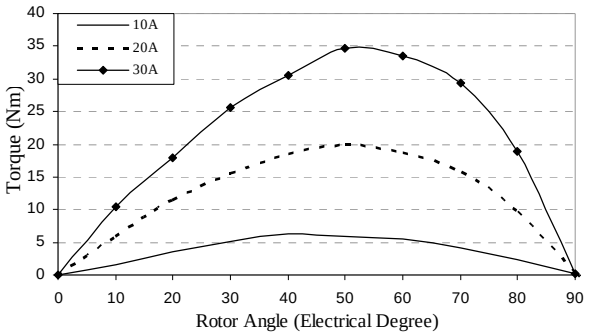

Figure 9. Measured torque versus rotor angle curves of proposed motor for different current values

The static torque measurement results of the proposed motor are presented for the current values of 10 A, 20 A and 30 A in Fig. 9.

C. *Load Tests*

The second part of the experimental study for the proposed motor is operating the machine with the motor drive and realizing the load tests. Therefore the motor prototype was connected with an auxiliary DC generator on the test bench.

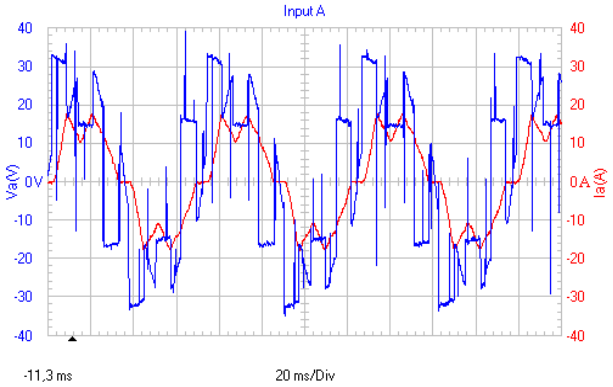

Figure 10. Experimental results of phase voltage and current waveforms at 9 Nm for the proposed motor

Bus voltage was chosen as 48 V for the motor drive and the motor was loaded up to maximum torque value allowed by the test set. Measured phase voltage and current waveforms are given in Fig. 10 for the proposed motor. Experimental speed versus torque curve is also shown in Fig. 12. The efficiency is also calculated as 82.4% from the measurement results at the load torque of 9 Nm.

VI. Results and Discussion

After completing FE analysis, simulations and experimental studies, the results can be gathered and discussed.

First, FE analysis can be compared to the measured torque versus rotor angle curves. Fig. 11 compares the measurement results with the results of FE analysis for the current values of 10 A, 20 A and 30 A. It can be seen from Fig. 11 that analysis and experimental studies give quite similar results at low current values. However, the difference between the results begins to increase along with the increase of the current value. In FE simulations, B-H curves of materials were defined in the program providing the curves of real materials used in the motor. So, simulation program takes into consideration the magnetic saturation according to the B-H curves. Although real B-H curves are used in existing FE software, there is a difference between simulated and measured torque waveforms, especially at high currents. Therefore, an advanced FE software environment can be used in order to include saturation effect exactly, in the future work. In addition, the difference may be due to the elasticity of the disc brake, the misalignment of the coupling and the motor prototype.

It is also seen from Fig. 11 that the maximum value of the produced torque does not increase linearly by the increase of the stator current. It shows that the magnetic flux in the machine is not constant and depends on the stator current. However it is affected by the saturation in the stator and rotor.

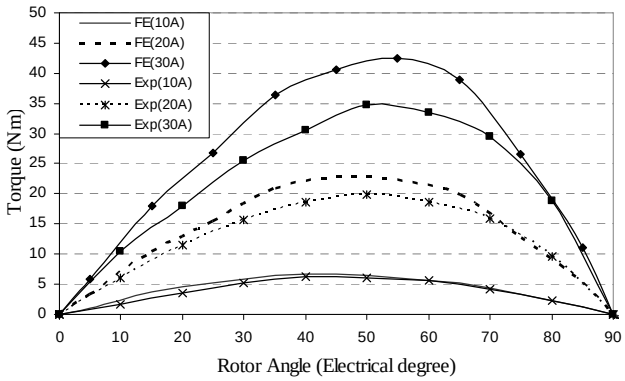

Figure 11. Comparison of torque waveforms of the proposed motor

Measured phase voltage and current waveforms in Fig. 10 accurately verify the simulation results in Fig. 6. It shows that the mathematical model of the motor and drive system agree well with the real system.

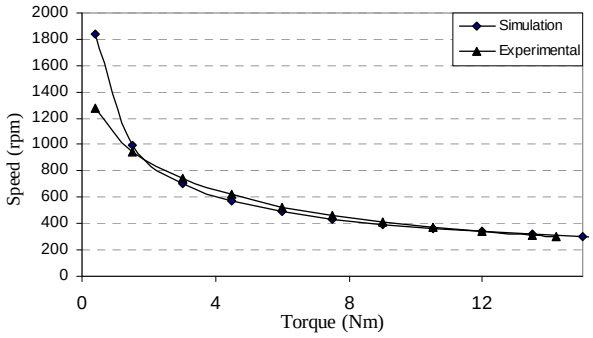

Figure 12. Comparison of speed versus torque curves

Speed versus torque curve comparison between simulation and experiment is given in Fig. 12. Due to the drive method, the characteristics resemble a DC series motor since the trend for the curve is exponential.

It is seen that the experimental results agree well with the numerical prediction. However, experimental value of the speed is lower than the simulated value for the proposed motor at low load torques. It can be explained as the motor speed reaches high at low or no loaded conditions since the stator current is small and machine magnetic flux is quite weak at this situation. Therefore small error in the calibration of the torque transducer can cause faulty in the measurements, especially at low torque conditions.

VII. CONCLUSION

An axially laminated motor construction has been presented in this study. FE analysis was first performed to predict the torque profiles and determine the rotor structure. Simulations were realized by the mathematical model of the motor system. Experimental studies were performed on a prototype motor to validate the FE analysis and simulations.

FE analysis shows that the thickness of both magnetic and non-magnetic materials is a significant parameter for the design process and skewing the stator slots makes a positive influence on the torque profiles. However, α_s should be chosen for an optimum value, because a small value of α_s does not affect the torque profile so much, whereas over skewing of the stator slots reduces the produced torque.

Measured torque waveforms are similar to the FE analysis. The results of the analysis and experiments show that variation of the maximum torque is not linear considering the increase of the stator current.

Proposed motor system was simulated and loaded tests were made at different torque values. The motor was operated with electrical 120° mode through synchronous operation of the motor drive with the position sensors. This mode is used in brushless DC motors and the control algorithm is quite easy. Speed of the motor can be varied by controlling the bus voltage of the motor drive. Measured and simulated phase voltage and current waveforms are quite similar.

Proposed motor differs from a switched reluctance motor since it has a distributed stator winding and an axially laminated reluctance rotor structure. It also differs from a brushless DC motor since it has no magnet material on the rotor.

When torque versus speed characteristic of the proposed motor is investigated, it is seen that the characteristic resembles a DC series machine. Therefore, the proposed motor can be used in variable-speed applications such as electrical vehicles in which the series characteristic and easy controllability of the motor speed is preferred.

REFERENCES

[1] D. A. Staton, T. J. E. Miller, and S. E. Wood, "Maximising the saliency ratio of the synchronous reluctance motor," *Proc. Inst. Elec. Eng. Electr. Power Appl.*, vol. 140, pp. 249–259, 1993.

[2] A. Vagati, M. Pastorelli, G. Franceschini, and S. C. Petrache, "Design of low-torque-ripple synchronous reluctance motors," IEEE Trans. Ind. Appl., vol. 34, pp. 758–765, Jul./Aug. 1998.

[3] Z. Wei, "Finite element computation of synchronous reluctance motor", *IEEE International Conference on Microwave Technology & Computational Electromagnetics*, Beijing, 2011, pp. 391 – 394.

[4] E.S. Obe, "Calculation of inductances and torque of an axially laminated synchronous reluctance motor", IET Electr. Power Appl., vol. 4, pp. 783–792, 2010.

[5] Y.-J. Luo, G.-J. Hwang, K.-T. Liu, "Design of synchronous reluctance motor", *Electrical Electronics Insulation Conference and Electrical Manufacturing & Coil Winding Conference*, Rosemont, IL, 1995, pp. 373-379.

[6] F. N. Isaac, A. A. Arkadan, A. A. Russel, and A. El-Antably, "Effects of anisotropy on the performance characteristics of an axially laminated anisotropic-rotor synchronous reluctance motor drive system", IEEE Transactions on Magnetics, vol. 34, pp. 3600–3603, Sept. 1998.

[7] W. L. Soong, D. A. Staton, and T. J. E. Miller, "Validation of lumped-circuit and finite-element modeling of axially-laminated brushless motors," *in Proc. Inst. Elec. Eng. 6th Int. Conf. Electrical Machines and Drives, EMD'93*, Oxford, 1993, pp. 85–90.

[8] D. A. Staton, T. J. E. Miller, and S. E. Wood, "Optimisation of the synchronous reluctance motor geometry," *5th Int. Conf. Electrical Machines and Drives*, pp. 156-160, 1991.

[9] R. Karimagako, M.H. Nagrial, J. Rizk, "Analysis and design of permanent magnet assisted synchronous reluctance machines", *5th IET International Conference on Power Electronics, Machines and Drives (PEMD 2010)*, Brighton, UK, 2010, pp. 1-6.

[10] P. Niazi, H.A. Toliyat, D.H. Cheong, J.C. Kim, "A low-cost and efficient permanent-magnet-assisted synchronous reluctance motor drive", IEEE Transactions on Industry Applications, vol. 43, pp. 542-550, 2007.

[11] P. Niazi., H.A. Toliyat, "Design of a low-cost concentric winding permanent magnet assisted synchronous reluctance motor drive", *IEEE 40th IAS Annual Meeting*, Kowloon, HongKong, 2005, pp. 1744-1748.

[12] E. Schmidt and W. Brandl, "Comparative finite element analysis of synchronous reluctance machines with internal rotor barriers," in *Proc. IEMDC*, Cambridge, MA, 2001, pp. 831–837.

[13] A. Vagati, M. Canova, M. Chiampi, M. Pastorelli, M. Repetto, "Design refinement of synchronous reluctance motors through finite-element analysis", IEEE Transactions on Industry Applications, vol. 36, 2000, pp. 1094–1102, 2000.

[14] A. Vagati, M. Canova, M. Chiampi, M. Pastorelli, M. Repetto, "Improvement of synchronous reluctance motor design through finite-element analysis", *in IAS Annu. Meeting Conf. Rec.*, Phoenix, AZ, 1999, pp. 862-871.

[15] N. Bianchi, B.J. Chalmers, "Axially laminated reluctance motor: Analytical and finite-element methods for magnetic analysis", IEEE Transactions on Magnetics, vol. 38, pp. 239-245, 2002.

[16] N. Bianchi and B. J. Chalmers, "Effect of the distribution of the laminations in an axially laminated reluctance motor," *in Proc. Inst. Elec. Eng. 9th Int. Conf. Electrical Machines and Drives, EMD'99*, Canterbury, U.K., 1999, pp. 376–380.

[17] N. Al-Aawar, A.A. Hanbali, A.A. Arkadan, "A novel approach for characterization and optimization of ala rotor synchronous reluctance motor drives for traction applications", *IEEE Vehicle Power and Propulsion Conference*, 2005, pp.327-333.

[18] B.J. Chalmers, L. Musaba, "Design and field-weakening performance of a synchronous reluctance motor with axially laminated rotor", IEEE Transactions on Industry Applications, vol. 34, pp. 1035-1041, 1998.

[19] T. Matsuo, T.A. Lipo, "Rotor design optimization of synchronous reluctance motor", IEEE Trans. Energy Convers., vol. 9, pp. 359–365, 1994.

[20] B. J. Chalmers and L. Musaba, "Design and field-weakening performance of a synchronous reluctance motor with axially-laminated rotor," *in IAS Annu. Meeting Conf. Record*, New Orleans, LA, 1997, pp. 271–278.

[21] I. Boldea, Z.W. Fu, S.A. Nasar, "Performance evaluation of axially-laminated anisotropic (ALA) rotor reluctance synchronous motors", IEEE Trans. Ind. Appl., vol. 30, pp. 977–985, 1994.

[22] T.A. Lipo, A. Vagati, L. Malesani, T. Fukao,, "Synchronous reluctance machines - A viable alternative for ac drives", *Ind. Appl. Society Annual Meeting Tutorial*, Oct. 1992.

[23] W.L. Soong, D.A. Staton, T.J.E. Miller, "Design of a new axially-laminated interior permanent magnet motor", IEEE Transactions on Industry Applications, vol. 31, pp. 358-367, 1995.

[24] W. L. Soong, D. A. Staton, and T. J. Miller, "Design of a new axially-laminated interior permanent magnet motor," *in Proc. IEEE IAS Annu. Meeting*, Toronto, 1993, pp. 27–36.

[25] I. Boldea I., S. Nasar, "Emerging electric machines with axially laminated anisotropic rotors: a review", Electrical Machines and Power Systems, vol. 19, pp. 673-704, 1991.